Proceedings of Symposia in Applied Mathematics
Volume **67.2**, 2009

Entropy stability of Roe-type upwind finite volume methods on unstructured grids

Aziz Madrane and Eitan Tadmor

Abstract. One reason which makes Roe's Riemann solver attractive is its low computational cost. But the main drawback with Roe's approximate Riemann solver is that non-physical expansion shocks can occur in the sonic points, it has been early remarked that for this particular situation. The Roe flux does not satisfy the entropy condition. In this paper an elegant response has been proposed by combining Harten and Tadmor entropy correction, with tuning parameters that play in fact the role of an artificial viscosity. Convergence and consistency with the entropy condition are proved. Numerical results on a two–dimensional hypersonic flow around a blunt body and double ellipsoïd confirm the theoretical results.

1. Introduction

The Roe flux replaces the nonlinear waves of the gas dynamics, i.e. the rarefactions and the shock waves by linear waves that are the contact discontinuities.If sufficiently weak shock waves occur for a given discontinuity between two states U_{left} and U_{right}, the Roe flux presented above is a good approximation, but if a rarefaction containing a sonic point is present among the nonlinear waves that solves the discontinuity problem between U_{left} and U_{right}, it has been remarked that for this particular situation, the Roe flux does not satisfay the entropy condition see Godlewski and Raviart [**GR**].

A popular response has been proposed by Harten and Hyman [**HH**], Van–Leer [**LPV**] and Yee [**Y**] with a tuning parameter that plays in fact the role of an artificial viscosity, but we observed problems at the stagnation point. An another entropy correction introduced by Tadmor [**T**], but this original version didn't give a best result at stagnation point for high speed flow.

In this paper we proposed the combination of Harten and Hyman [**HH**] and Tadmor [**T**] entropy correction, we observed the solution is better at stagnation point and the scheme is not more diffusive, but there is two parameter to control.

2. Mathematical modelling

2.1. Governing equations. In the sequel, we consider domains of computation related to external flows around bodies; in (fig.1), the body is represented as a double ellipsoïd which limits the domain of computation by its wall Γ_B.

Let $\Omega \subset \mathbb{R}^2$ be the flow domain of interest and Γ be its boundary, we write $\Gamma = \Gamma_B \cup \Gamma_\infty \cup \Gamma_E$, where Γ_B denotes that part of the body boundary which is relevant for the computational domain (fig.1).
Γ_∞ is the (upwind) farfield boundary, and $\Gamma_E = \Gamma_E^1 \cup \Gamma_E^2$ is the (downwind) exit part of the boundary. The equations describing two-dimensional compressible inviscid

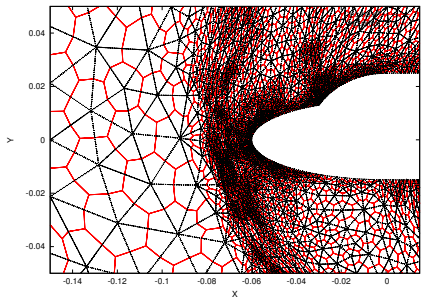

FIGURE 1. Boundary of the computational domain, primary grid and barycentric cells

flows are the Euler equations, written here in their dimensionless form [**PT**], given by

$$\frac{\partial}{\partial t}U(x,y;t) + \frac{\partial}{\partial x}F(U(x,y;t)) + \frac{\partial}{\partial y}G(U(x,y;t)) = 0\,, \quad (x,y;t) \in \Omega \times R^+ \tag{2.1}$$

Let ρ, u, v, p, E, c and M denote the density, velocity components, pressure, total energy, speed of sound and Mach number. For a perfect gas the pressure the speed of sound and the Mach number are given by

$$p = (\gamma - 1)(\rho E - \frac{1}{2}\rho(u^2 + v^2)) \quad c = \sqrt{\frac{\gamma p}{\rho}}\,, \quad M = \frac{\sqrt{u^2 + v^2}}{c}\,.$$

2.2. Boundary conditions. The flow is assumed to be uniform at the farfield boundary Γ_∞ and we impose

$$\rho_\infty = 1, \quad \overrightarrow{V}_\infty = \begin{pmatrix} cos\alpha \\ sin\alpha \end{pmatrix}, \quad p_\infty = \frac{1}{\gamma M_\infty^2} \tag{2.2}$$

where α is the angle of attack and M_∞ denotes the free-stream Mach number.On the wall boundary Γ_B, we assume $\overrightarrow{V} \cdot \overrightarrow{n}_{|\Gamma_B} = 0$. Finally, for unsteady calculations, an initial flow, $U(x,0) = U_0(x)$, is prescribed on Ω.

3. Space and time discretization

3.1. Definitions. We assume that Ω is a bounded polyhedral domain of $\mathbb{R}^2$. We introduce a FEM triangulation $\mathcal{T}_h$ in $\mathbb{R}^2$, where h is the maximal length of the edges in $\mathcal{T}_h$. With the property that the intersection of two triangles is either empty or consists of one common vertex or side. for the primary grid see (fig. 2), the nodes are the vertices a_i of the triangle $\tau \in \mathcal{T}_h$, and the finite volume cells are the barycentric cells C_i, obtained by joining the midpoints M_{ij} of the sides originating at node a_i to the centroids G_{ij} of the triangle of $\mathcal{T}_h$ which meet at a_i see (fig. 2). In the sequel we use the following notation.

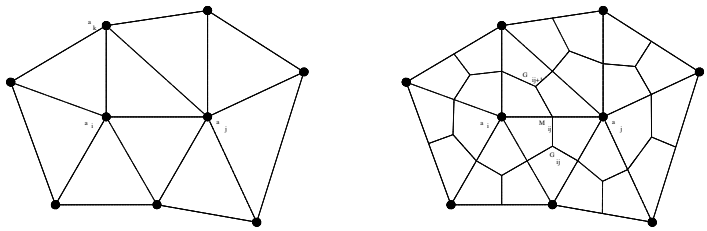

FIGURE 2. Primary grid and barycentric cells

NOTATION 1. *Let a_i, a_j, a_k be the three nodes defining a teriangle τ, $\tau \in \mathcal{T}_h$. Then*

- a_i *is the i^{th} vertex*
- M_{ij} *is the midpoint of side $a_i a_j$*
- n_i *is the number of the nodes which are adjacent to a_i*
- $K(i)$ *is the set of nodes (vertices) which are neighbors of node a_i, $G_{ij}(j = 1, \ldots, n_i)$ is the barycenter of a triangle of which a_i is a vertex*
- C_i *is the barycentric cell constructed around a_i*
- Γ_{ij} *is the cell boundary element $G_{ij}M_{ij}G_{i,j+1} = \partial C_i \cap \partial C_j = \partial C_{ij}$ (see fig. 2)*
- $\partial C_i = \bigcup_{j=1}^{n_i} \Gamma_{ij}$ *is the boundary of cell C_i*
- $\vec{\nu}_i = (\nu_{i_x}, \nu_{i_y})$ *is the unit outward normal vector to ∂C_i.*

Let $U_i^n \cong U(a_i, t^n)$ denote the nodal cell average values at time $t = t^n$. The union of all the barycentric cells constitutes a partition of the computational domain Ω_h, $\Omega_h = \bigcup_{i=1}^{\text{nv}} C_i$, where nv is the number of vertices of the original finite element triangulation $\mathcal{T}_h$.

3.2. Finite volume formulation on unstructured grids. The space discretization method considered here,combine the following elements:

- a vertex centered finite volume formulation involving upwind schemes for the calculation of the convective fluxes.
- a MUSCL [**V**] technique for the extension to second order accuracy in the calculation of the convective fluxes.

In order to set the appropriate frame for the discrete problem which will be solved to approximate the solution of the original problem, we introduce the following **discrete spaces** .

$$\mathcal{V}_h = \{v_h | v_h \in L^2(\Omega), v_h|_{C_i} = v_i = const; \;\; i = 1, \cdots, nv\} \tag{3.1}$$

A general variational formulation of equation (2.1) can be written as:

Find $U_h \in (\mathcal{V}_h)^4$
such that

$$\int_{\Omega_h} \frac{\partial U_h}{\partial t} \varphi_h dxdy + \int_{\Omega_h} \overrightarrow{\nabla} \cdot \overrightarrow{\mathcal{F}}(U_h) \varphi_h dxdy = 0 \quad \forall \;\; \varphi_h \in \mathcal{V}_h \tag{3.2}$$

Where φ_h is the characteristic function of the control volume C_i, which is such that $\varphi_h = 1$ on cell C_i, and 0 elsewhere.

Equation (3.2) can be written as follow:

$$\int_{Supp\varphi_h=C_i}[\frac{\partial U_h}{\partial t}+\overrightarrow{\nabla}\cdot\overrightarrow{\mathcal{F}}(U_h)]dxdy=0 \quad \forall \quad i=1,nv \tag{3.3}$$

Applying Green's formula to the convective terms of (3.3), we obtain

$$\int_{C_i}\frac{\partial U_h}{\partial t}dxdy+\int_{\partial C_i}\overrightarrow{\mathcal{F}}(U_h)\cdot\overrightarrow{\nu_i}d\sigma=0 \tag{3.4}$$

Observing that

$$\partial C_i=\bigcup_{j\in K(i)}\{\partial C_i\cap\partial C_j\}\cup\{\partial C_i\cap\Gamma_B\}\cup\{\partial C_i\cap\Gamma_\infty\}$$

we thus get

$$\begin{aligned}&\text{Area}(C_i)(U_i^{n+1}-U_i^n)+\Delta t\sum_{j\in K(i)}\int_{\partial C_i\cap\partial C_j}\overrightarrow{\mathcal{F}}(U(\vec{x},t^n)\cdot\vec{\nu_i}\,d\sigma\\&+\Delta t\int_{\partial C_i\cap\Gamma_B}\overrightarrow{\mathcal{F}}(U_h^n)\cdot\vec{\nu}\,d\sigma+\Delta t\int_{\partial C_i\cap\Gamma_\infty}\overrightarrow{\mathcal{F}}(U_h^n)\cdot\vec{\nu}\,d\sigma=0\end{aligned} \tag{3.5}$$

In this study, the convective terms of (3.5) are computed using upwind schemes that are well adapted for the hyperbolic nature of the system of Euler equations.

A conservative and consistant finite volume approximation of (3.5) is written

$$\begin{aligned}&\text{Area}(C_i)(U_i^{n+1}-U_i^n)+\Delta t\sum_{j\in K(i)}\Phi(U_i,U_j,\vec{\nu_{ij}})\\&+\Delta t\int_{\partial C_i\cap\Gamma_B}\overrightarrow{\mathcal{F}}(U_h^n)\cdot\vec{\nu}\,d\sigma+\Delta t\int_{\partial C_i\cap\Gamma_\infty}\overrightarrow{\mathcal{F}}(U_h^n)\cdot\vec{\nu}\,d\sigma=0\end{aligned} \tag{3.6}$$

where Φ denotes a numerical flux function which is such that

$$\left\{\begin{array}{lcl}\Phi(U_i,U_j,\vec{\nu_{ij}}) & = & -\Phi(U_i,U_j,-\vec{\nu_{ij}})\\ \Phi(U_i,U_j,\vec{\nu_{ij}}) & = & \displaystyle\int_{\partial C_i\cap\partial C_j}\overrightarrow{\mathcal{F}}(U(\vec{x},t^n)\cdot\vec{\nu_i}\,d\sigma\approx\overrightarrow{\mathcal{F}}(U(x_{\vec{M}_{ij}},t^n)\cdot\vec{\nu_{ij}}\end{array}\right. \tag{3.7}$$

Where

$$\vec{\nu_{ij}}=\int_{\partial C_i\cap\partial C_j}\vec{\nu}\,d\sigma=\vec{\nu_{ij}^1}+\vec{\nu_{ij}^2} \tag{3.8}$$

Let A, B denote the Jacobian matrices $\partial F(U)/\partial U$, $\partial G(U)/\partial U$, respectively. Then Eq. (2.1) can be written in the nonconservative form:

$$\frac{\partial U}{\partial t}+\overrightarrow{\mathcal{F}}'(U)\cdot\nabla U=\frac{\partial U}{\partial t}+A(U)\,\frac{\partial U}{\partial x}+B(U)\,\frac{\partial U}{\partial y}=0. \tag{3.9}$$

One possible way to compute the numerical flux Φ_{ij} at the interface between two control volumes is based on the solution of a local one–dimensional Riemann problem defined at the interface $\partial C_i\cap\partial C_j$:

$$\left\{\begin{array}{l}U_t+\vec{\nabla}.\overrightarrow{\mathcal{F}}(U).\boldsymbol{n}=0\\ \\ U(x,y;0)=\left\{\begin{array}{ll}U_l & \text{if } \boldsymbol{X}.\boldsymbol{n}<0\\ \\ U_r & \text{if } \boldsymbol{X}.\boldsymbol{n}>0\end{array}\right. \quad \text{with} \quad \boldsymbol{X}=\left(\begin{array}{c}x\\y\end{array}\right)\end{array}\right. \tag{3.10}$$

where U_l and U_r are two states given at the left and the right sides of $\partial C_i \cap \partial C_j$, In practice this Riemann problem is often solved approximately using Riemann solvers.The method adopted in this study has been proposed by Roe [**R**].It consists in approximating the solution of the Riemann problem (3.10) throught the linearization of the term $\vec{\nabla}.\overrightarrow{\mathcal{F}}(U).\boldsymbol{n}$ which is replaced by $\mathcal{A}_{ij}\frac{\partial U}{\partial \boldsymbol{n}}$ where $\mathcal{A}_{ij}$ is a shorthand notation for $\mathcal{A}_{ij}(U_l, U_r, \vec{\nu_{ij}})$. $\mathcal{A}_{ij}$ is the Jacobian Matrix of Roe which is such that it :

- preserves the hyperbolicity of the original system of PDEs system that is the diagonalization of $\mathcal{A}_{ij}$ results in real eigenvalues and linearly independant eigenvectors;
- is consistant with the Jacobian matrix $\frac{\partial \overrightarrow{\mathcal{F}}(U)}{\partial U}$

$$\mathcal{A}_{ij} = \mathcal{A}_{ij}(U_i, U_i, \vec{\nu_{ij}}) = \frac{\partial \overrightarrow{\mathcal{F}}(U_i)}{\partial U}$$

- insures a conservation principle through discontinuities:

$$(\overrightarrow{\mathcal{F}}(U_i) - (\overrightarrow{\mathcal{F}}(U_j)).\vec{\nu_{ij}} = \mathcal{A}_{ij}(U_i, U_j, \vec{\nu_{ij}})(U_i - U_j)$$

In practice, the Jacobian matrix that characterizes Roe's scheme is evaluated as:

$$\mathcal{A}_{ij}(\widetilde{U_{ij}}) = \frac{\partial \overrightarrow{\mathcal{F}}(U)}{\partial U}(\widetilde{U_{ij}}, \vec{\nu_{ij}})$$

where $\widetilde{U_{ij}}$ is Roe average between a state U_i and U_j.

$$\Phi_{ij} = \Phi(U_i, U_j, \nu_{ij}) = \frac{1}{2}(\overrightarrow{\mathcal{F}}(U_i) + (\overrightarrow{\mathcal{F}}(U_j)).\vec{\nu_{ij}} - \frac{1}{2}d\,(U_i, U_j, \vec{\nu_{ij}}) \tag{3.11}$$

where $d\,(U_i, U_j, \vec{\nu_{ij}})$ corresponds to a numerical diffusion term:

$$d\,(U_i, U_j, \vec{\nu_{ij}}) = |\mathcal{A}(\widetilde{U_{ij}}, \vec{\nu_{ij}})| \cdot (U_i - U_j)$$

We verify (see [**DM**]) that the Roe flux can be rewritten as follow:

$$\Phi_{ij} = \Phi(U_i, U_j, \vec{\nu_{ij}}) = \frac{1}{2}(\overrightarrow{\mathcal{F}}(U_i) + (\overrightarrow{\mathcal{F}}(U_j)).\vec{\nu_{ij}} - \frac{1}{2}\sum_{k=1}^{4}|\lambda_k(U_i, U_j)|\boldsymbol{r}_k(U_i, U_j) \tag{3.12}$$

where $\boldsymbol{r}_k(U_i, U_j)$ and $\lambda_k(U_i, U_j)$ are the eigenvectors and associated eigenvalues of the Jacobian matrix $\mathcal{A}(\widetilde{U_{ij}}, \vec{\nu_{ij}})$.

3.2.1. *Treatment of the boundary fluxes:* We shall use the following approximation for the

Farfield boundary integral Γ_∞:

$$\int_{\partial C_i \cap \Gamma_\infty} \overrightarrow{\mathcal{F}(\mathcal{U})}_h \cdot \overrightarrow{n}_i d\sigma = \mathcal{A}^+(U_i, \overrightarrow{\nu}_{i\infty}) \cdot U_i + \mathcal{A}^-(U_i, \overrightarrow{\nu}_{i\infty}) \cdot U_\infty$$

where $\mathcal{A}$ is the flux Jacobian matrix of $\frac{\partial \overrightarrow{\mathcal{F}}(U)}{\partial U} \cdot \overrightarrow{\nu} = \frac{\partial F}{\partial U}\nu_x + \frac{\partial G}{\partial U}\nu_y$, and $\mathcal{A}^+, \mathcal{A}^-$ are the positive and negative parts of $\mathcal{A}$, respectively.

Wall boundary integral Γ_B: Taking into account the slip boundary condition $\overrightarrow{V} \cdot \overrightarrow{n}_{|\Gamma_B} = 0$. We see that the only contribution to the exact flux comes from the

pressure

$$\int_{\partial C_i \cap \Gamma_B} \overrightarrow{\mathcal{F}(\mathcal{U})}_h \cdot \overrightarrow{n}_i d\sigma = \int_{\partial C_i \cap \Gamma_B} \begin{pmatrix} 0 \\ p_i \nu_x \\ p_i \nu_y \\ 0 \end{pmatrix} d\sigma$$

3.2.2. **Time step size:** The local time stepping has been used and controlled by the formula, for each cell C_i, full details will be provided in [**MT**] :

$$\Delta t_i = CFL \frac{\text{Area}(C_i)}{\lambda^i_{\max} \int_{\partial C_i} d\sigma}$$

with

$$\lambda^i_{\max} = \max(\lambda_i, \max_{j \in K(i)} \lambda_j), \qquad \lambda_i = (u_i^2 + v_i^2)^{\frac{1}{2}} + c_i$$

$$\Delta t = \min_{i=1,nv} \Delta t_i$$

3.2.3. **Second order reconstruction, approximation of the slopes and limitation:** The numerical computation of the convective flux using (3.11) is first order in space. To be more accurate, the interplolated states U_{ij} and U_{ji} are defined as [**V**]:

$$\begin{cases} U_{ij} = U^l = U_i^n + \nabla U_i^n \cdot (\vec{x}_i - \vec{x}), & \forall \vec{x} \in C_i,\ \vec{x} \in \mathbb{R}^2. \\ \\ U_{ji} = U^r = U_j^n + \nabla U_j^n \cdot (\vec{x}_j - \vec{x}), & \forall \vec{x} \in C_j,\ \vec{x} \in \mathbb{R}^2. \end{cases} \tag{3.13}$$

where $U = (\rho, u, v, p)^T$, in other words, the interpolation is done using the physical variables instead of the conservative variables. The interpolated states (3.13) are used as arguments to the numerical flux function (3.11).
In order to compute the gradient ∇U_i^n of the piecewise linear interpolant for the cell C_i, we use Green–Gauss' method [**BJ**].For the limitation we use [**VV**].

3.3. A modified Roe-scheme. For general hyperbolic systems, the existence of mathematical entropy ensures the existence of the Roe-type linearization (see [**HLV**]). It is well known fact that such a linearization is not unique and that Roe's scheme does not satisfy the entropy inequality. This is one of the serious drawback of the Roe's method.

3.3.1. *Harten entropic correction.* Harten showed that the solution verifies the entropy condition if the Roe fluxes (3.11) are modified in the following way:
(3.14)

$$\Phi_{ij} = \Phi(U_{ij}, U_{ji}, \nu_{ij}) = \frac{1}{2}(\overrightarrow{\mathcal{F}}(U_{ij}) + (\overrightarrow{\mathcal{F}}(U_{ji})).\vec{\nu_{ij}} - \frac{1}{2} \sum_{k=1}^{4} Q^{\mathrm{H}}(\lambda_k(U_{ij}, U_{ji})) \boldsymbol{r}_k(U_{ij}, U_{ji})$$

where the function Q^{H} is defined by (see fig. 3)

$$|a|^\star = Q^{\mathrm{H}}(a) = \begin{cases} |a| & \text{if } |a| > \dfrac{\delta^\star}{2} \\ \\ \dfrac{a^2}{\delta^\star} + \dfrac{\delta^\star}{4} & \text{if } |a| \leq \dfrac{\delta^\star}{2} \end{cases} \tag{3.15}$$

Various choices of δ^* can be found in the literature, e.g., [**Y**]

$$\delta^* \quad = \quad \delta(u + v + c),\ 0.1 \leq \delta \leq 0.5, \tag{3.16}$$

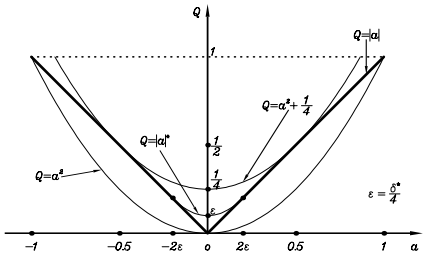

FIGURE 3. Function Q^{H} of the Harten correction

where $\Delta a = a_R - a_L$ is the difference between the values of a on the righthand and lefthand sides of the edge, u, v are the two components of the velocity and c is the speed of sound.
We have tested an other entropy correction introduced by Tadmor [**T**]. The original version

$$Q^{\mathrm{Tad}}(a) = |a| + \max\left(\frac{1}{6}\Delta a + K\,|\Delta u|^2\,;\,0\right)\ ,\quad K>0 \tag{3.17}$$

didn't give a best result at stagnation point see (fig. 5). But, if we combine (3.15) and (3.17)

$$Q^{\mathrm{HHT}}(a) = |a|^* + \max\left(\frac{1}{6}\Delta a + K\,|\Delta u|^2\,;\,0\right)\ ,\quad K>0 \tag{3.18}$$

where $|a|^*$ is obtained by using the entropy correction of the form (3.15,3.16), the solution become acceptable at stagnation point see (fig. 6), by increasing the parameters δ and K, we obtain better solution see (fig. 7). The above entropic correction are equivalent to introducing a certain amount of artificial viscosity, the exact amount depending on a parameter which requires a case-dependent adjustment.

4. Numerical experiments

The present section discusses computational results for a standard finite volume scheme, which is formulated for meshes composed by unstructured triangles. The objective of the present study is to make comparison of different entropic corrections and to assess its advantages and disadvantages. Hence the test cases here are selected among for which the solutions well documented, independent data are available in the literature [**IGS**] and [**PI**].

4.1. Flow over a blunt body at 0^o of angle of attack and $M_\infty = 20$. The first test case presented considers the hypersonic flow over a 2-D blunt body with freestream Mach number $M_\infty = 20.$ and angle of attack $\alpha^o = 0.$. The perfect gas hypothesis is assumed, despite the high Mach numbers appearing in the studied flows. The aim of this test is to verify the behaviour of the second order finite volume method on unstructured grids with the relation to the appearance of the carbuncle phenomenon . The carbuncle phenomenon is characterized by the appearance of a spurious disturbance behind a detached shock wave that forms overs blunt bodies. Such a numerical problem presents a stable solution which includes a recirculation bubble situated in front of the stagnation region of the flow. In the present test case, a mesh with 9151 triangles and 4695 points is used. Results for a cut at $y = 0$

of Mach number are shown in figs. (4, 5, 6), showing good shock–capturing. For the choices of (3.15,3.16), (3.17) and (3.18) with a small parameters δ and K we observe problems at the stagnation point,see (figs. 4, 5, 6). On the other hand, if we increase δ and K, $\delta = 0.5$ and $K = 0.5$ the solution is getting better at the stagnation point see (fig. 7).

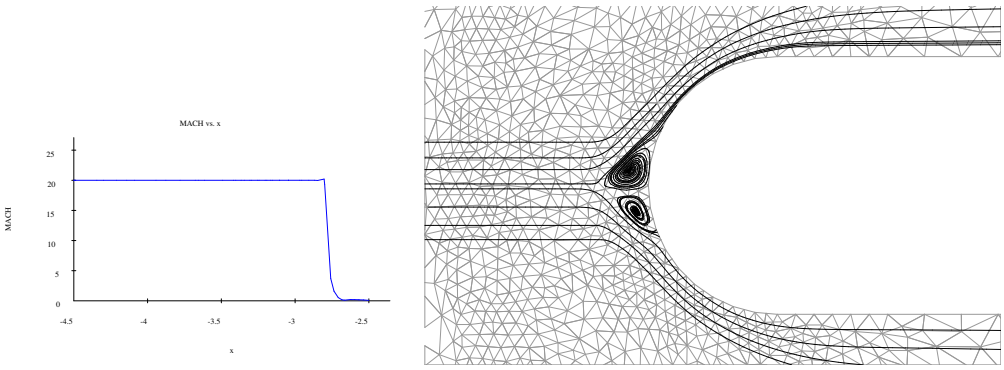

FIGURE 4. Cut at $y = 0$ of Mach number and streamlines obtained with entropy fix (3.15,3.16), $\delta = 0.2$

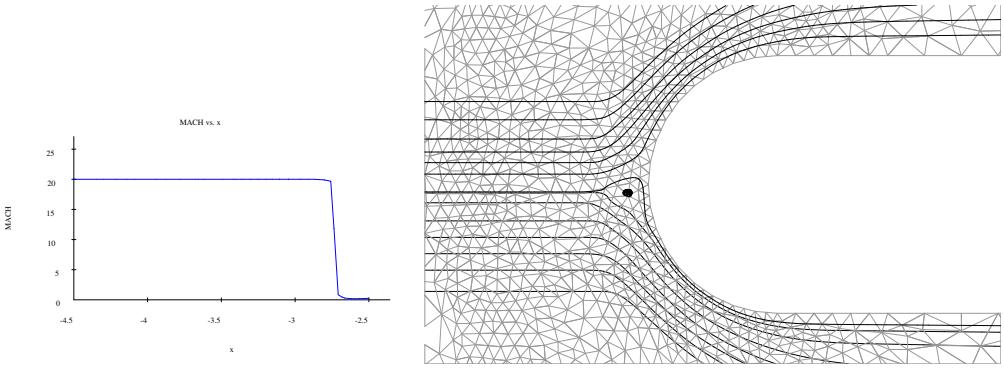

FIGURE 5. Cut at $y = 0$ of Mach number and streamlines obtained with entropy fix 3.17), $K = 0.2$)

4.2. Flow past a double ellipsoïd at 0^o of angle of attack and $M_\infty = 8.15$. For this problem inspired by ([**IGS**]), with Mach number $M_\infty = 8.15$ and 0^o of angle of attack. The mesh has 2928 triangles and 1558 points, see (fig. 1). We restrict our choice to (3.18) and (3.17). we observe problems at the stagnation point for (3.17), see (fig. 8), but the solution is getting better at the stagnation point for (3.18), see (figs. 9).

5. Conclusion and perspectives

The feasibility of the finite volume method approximation was demonstrated on flow around a double ellipsoïd and blunt body when using unstructured triangular grids. The computational experiments show us, the combination of Harten and Tadmor correction is good and robust approach for high speed flow.

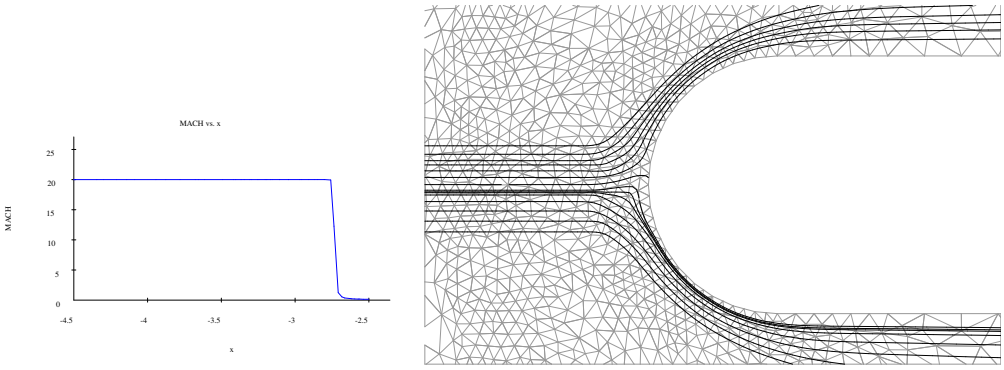

FIGURE 6. Cut at $y = 0$ of Mach number and streamlines obtained with entropy fix (3.18) and (3.17), $\delta = K = 0.2$

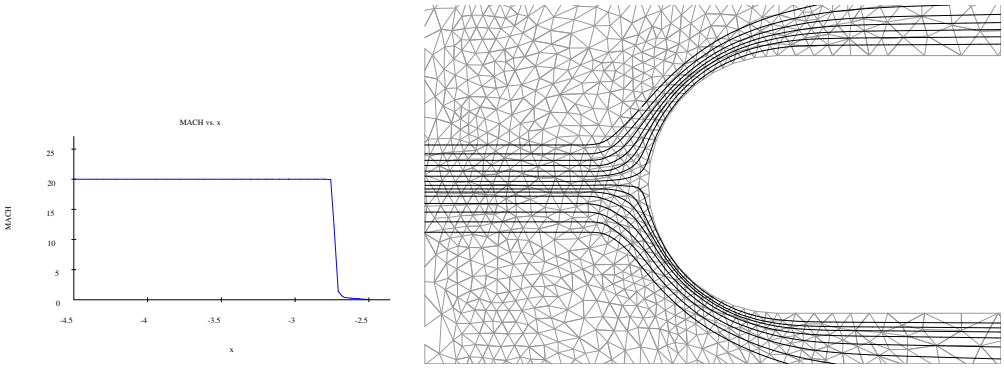

FIGURE 7. Cut at $y = 0$ of Mach number and streamlines obtained with entropy fix (3.18) and (3.17), $\delta = K = 0.5$

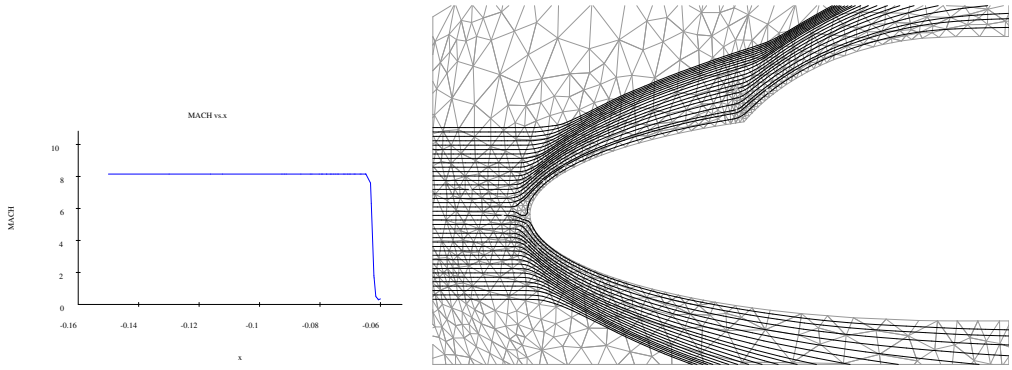

FIGURE 8. Mach contours obtained with entropy fix (3.17), $K = 0.5$)

References

[BJ] T.J. BARTH AND D.C. JESPERSEN, *The design and application of upwind schemes on unstructured meshes*, AIAA Paper No. 89-0366, 27th Aerospace Sciences Meeting, January 9–12, 1989, Reno, Nevada, 1989.

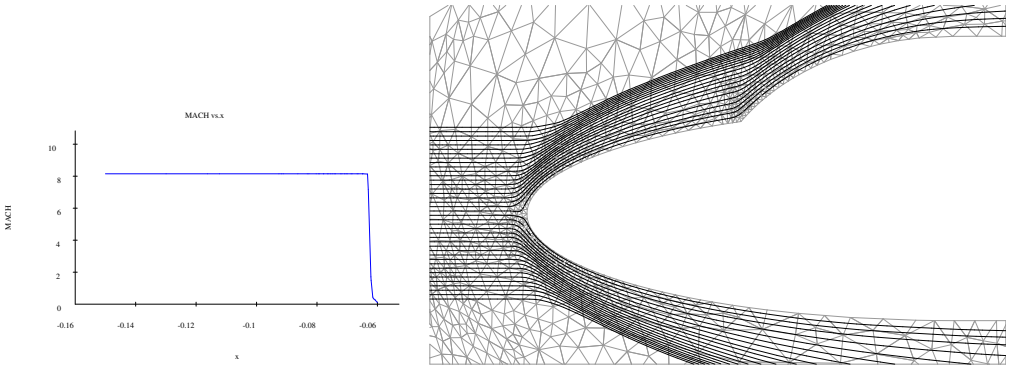

FIGURE 9. Mach contours obtained with entropy fix (3.18) and (3.17), $\delta = K = 0.5$

[DM] F. DUBOIS, G. MEHLMANN *A non–parameterized entropy correction for Roe's approximate Riemann solver*,Numerische Mathematik,73, pp. 169–208, (1996).

[GR] E. GODLEWSKI AND P.A. RAVIART, *Numerical Approximation of Hyperbolic Systems of Conservation Laws*, Springer-Verlag, 1996.

[HH] A. HARTEN AND J. HYMAN, *Self-adjusting grid method for one dimensional hyberbolic conservation laws*,Journal of Computational Physics, 50 (1983), pp. 235–269.

[HLV] A. HARTEN, P.D. LAX, B. VAN LEER, *On Upstream Differencing and Godunov–type schemes for Hyperbolic Conservation Laws*, SIAM Review 25, pp. 35–61.

[IGS] INRIA AND GAMNI-SMAI (1990), *Workshop on hypersonic flows for reentry problems, Problem 6 : Flow over a double ellipse, test case 6.1 : Non-Reactive Flows. Antibes*, France, January 22-25, 1990.

[LPV] D.W.LEVY, K.G. POWELL AND B. VAN–LEER *An implementation of a grid independant upwind scheme for the Euler equations*, AIAA paper, 89–1931 (1989).

[MT] A. MADRANE AND E. TADMOR *Entropy stability of Roe-type upwind finite volume methods on unstructured grids*, in preparation.

[PI] K.M. PERRY AND S.T. IMLAY, *Blunt body flow simulations*, 24th AIAA Joint Propulsion Conference, AIAA paper No 88-2904, Boston, MA, 1988.

[PT] R. PEYRET AND T.-D. TAYLOR, *Computational Methods for Fluid Flow*, Springer-Verlag, New York, Heidelberg, Berlin, 1983.

[R] P. L. ROE, *Approximate Riemann solver, parameter vectors, and difference schemes*,J. Comp. Phys.,43 (1981), pp. 357–372.

[T] E. TADMOR, *Entropy stability theory for difference approximations of nonlinear conservation laws and related time–dependant problem*, Acta Numerica (2003), pp. 451–512.

[V] B. VAN LEER, *Towards the ultimate conservative difference scheme V. A second-order sequel to Godunov's method*, J. Comp. Physics, 32 (1979), pp. 101–136.

[VV] V. VENKATAKRISHNAN, *Convergence to steady state solutions of the Euler equations on unstructured grids with limiters*, J. Comp. Phys. 118 (1995), pp. 120–130.

[Y] H.C. YEE, *A class of high–resolution explicit and implicit shock–capturing methods*, Lecture Series Von Karman Institute for Fluid Dynamics, 04 (1989). In Computational Fluid Dynamics.

AIRBUS/IAT, FLUGHAFENALLEE 10, D-28199 BREMEN, GERMANY.
E-mail address: aziz.madrane@airbus.com

DEPARTMENT OF MATHEMATIC CENTER FOR SCIENTIFIC COMPUTATION AND MATHEMATICAL MODELING INSTITUTE FOR PHYSICAL SCIENCE & TECHNOLOGY UNIVERSITY OF MARYLAND,COLLEGE PARK,MD,USA.
E-mail address: tadmor@cscamm.umd.edu